ОБЪЕДИНЕННЫЙ
ИНСТИТУТ
ЯДЕРНЫХ
ИССЛЕДОВАНИЙ

Дубна

E9-96-128

I.V.Kalagin, V.P.Ovsyannikov

NUMERICAL SIMULATION OF ION PRODUCTION PROCESSES IN EBIS

Submitted to «Nuclear Instruments and Methods»

1996

Introduction

The electron-beam method of multicharge ion production was suggested by E.D.Donets in 1967 /1/. The first attempt to create an Electron-Beam Ion Source (EBIS) theory was undertaken by R.Becker / 2/ and M.C.Vella in 1981/3/. A more complete theory of the electron-beam method of multicharge ionization in an ion trap was created by the Livermore EBIT group (M.Levine, M.Penetrante, R.Marrs et al.) /4,5/. Based on these results, we present a simpler numerical model of multicharge ionization in EBIS. Simplifications follow from our previous papers/6,7/. The computer codes describing the Kryon-S experimental data can be used to predict EBIS basic parameters: charge state spectrum, ion-beam current and even ion beam emittance.

Physical processes in the trap

According to the Livermore papers, main processes in the EBIS trap are the following:

-electron-impact ionization of ions,
-radiative recombination of ions,
-charge exchange between ions and neutral atoms,
-ion heating by an electron beam,
-ion-ion energy exchange,
-ion confinement in the trap,
-ion escape from the trap.

Electron-impact ionization

$$A + e^- \Rightarrow A^{K+} + (K+1)e^-,$$

where K=1,2... .

To calculate single step (K=1) ionization cross-section, the empirical Lotz formula is used /8,9/:

$$\sigma_{i\to i+1} = \sum_{l=1}^{N} a_l q_l \frac{\ln(E_e / P_l)}{E_e P_l}\left\{1 - b_l \exp\left[-c_l\left(E_e / P_l - 1\right)\right]\right\} ; \qquad (1)$$

where $E_e \geq P_l$, N is the number of subshells in atom or ion, q_l is the number of electrons in an ith subshell, E_e is the electron energy, P_l is the binding energy for an ith subshell, a_l, b_l, c_l are constants. For Z>3, a_l=4.5·10^{-14} (cm^{2}eV^2) and b_l, c_l=0.

The ionization at K=2,.. takes place for outer shells as shown for M-shell of Ar/7,10/. But these processes cannot be taken into account for inner shells.

Radiative recombination

$$A^{K+} + e^- \Rightarrow A^{(K-1)+} + \nu,$$

The Kim and Pratt formula/11/ can be used for the recombination cross-section, but for EBIS with optimum electron-beam energy parameters radiative recombination processes are neglected.

Charge exchange

$$A^{K+} + B \Rightarrow A^{(K-1)+} + B^+,$$

In the EBIS case, charge exchange processes are the main concurrent to electron-impact ionization ones. The charge exchange cross-section is calculated using the Muller and Salzborn formula /12/:

$$\sigma_{i\to i-1} = 1.43\times10^{-12}\, Z_i^{1.17}\, P_0^{-2.76} , \qquad (2)$$

where Z_i is the ion charge and P_0 the ionization potential of the neutral target.

Ion heating by the electron beam

The electron energy loss is/14/:

$$\frac{dE_e}{dt} = -\frac{2m_e}{M_i} E_e \nu_m , \qquad (3)$$

where E_e is the electron energy, m_e the electron mass, M_i the ion mass, and ν_m the rate of electron-ion collisions: $\nu_m = N_i \sigma_{tr} \nu_e$,
where N_i is the ion density, V_e the electron speed, and σ_{tr} the Coulomb cross section:

$$\sigma_{tr} = 4\pi\left(\frac{Z_i e^2}{m_e}\right)^2 \frac{\ln\Lambda_i}{V_e^4} , \qquad (4)$$

with e the electron charge, Z_i the ion charge, and ln Λ_i the electron-ion Coulomb logarithm.

Energy is transferred via Coulomb collisions from electrons to ions for the rate:

$$\left[\frac{d(N_i kT_i)}{dt}\right]^{heating} \sim \left(-\frac{dE_e}{dt}\right)\cdot N_e \cdot N_i . \qquad (5)$$

where kT_i is the ion temperature.

Formula (5) is in accordance with the formula used by the Livermore group/5/.

Ion-ion energy exchange

The rate of energy gain of *i*th ionic species due to collisions with *j*th ionic species is written as /5/:

$$\left[\frac{d(N_i kT_i)_j}{dt}\right]^{exchange} = 2\nu_{ij} N_i \frac{Mi}{M_j} \frac{k(T_j - T_i)}{(1 + M_i T_j / M_j T_i)^{3/2}} \quad , \qquad (6)$$

where ν_{ij} is the Coulomb collision rate between *i*th and *j*th ionic species, kT_i, kT_j are the ionic temperatures of *i*th and *j*th species, and M_i, M_j are the ion masses,

$$\nu_{ij} = \frac{4}{3}\sqrt{2\pi} N_j \left(\frac{Z_i Z_j e^2}{M_i}\right)^2 \left(\frac{M_i}{kT_i}\right)^{3/2} \ln\Lambda_{ij} \ , \qquad (7)$$

with $\ln \Lambda_{ij}$ the ion-ion Coulomb logarithms.

Ion trapping

The radial potential on the electron beam edge relative to the beam axis reads as /4/:

$$V_b = 485 \frac{I_e}{\sqrt{E_e}} (1 - f) \quad (\mathrm{V}), \qquad (8)$$

where I_e is the electron beam current (A) and E_e the beam energy (keV),
Beam compensation: $f = \langle Z \rangle \cdot N_i / N_e$, (9)
Effective radial potential: $V_{eff} = k \cdot V_b$, (10)
with $1 \le k \le 2$.

Axial losses are prevented by high potential barriers installed at the boundary drift tube sections. The axial barrier voltage can be larger than the radial barrier one. This is the reason for considering radial losses only.

Ion escape from the trap

The Maxwell-Boltzman distribution function is the following /16/:

$$f_i(E_i) = \frac{2}{\sqrt{\pi}} \frac{1}{kT_i} \sqrt{E_i / kT_i} \exp(-E_i / kT_i), \qquad (11)$$

Let the function be normalized as:

$$\int_{E_i=0}^{\infty} f_i(E_i) dE_i = 1 \ , \qquad (12)$$

and the distribution be established for about $t_{min} \le 1/\nu_{ij}$, where $i=j$. As a rule, $t_{min} \le 1\mu s$ for the EBIS parameters: $N_i \ge 10^6$ cm^{-3}, $kT_i \ge 1$ eV.

The border energy for ions with charge Z: $E_b = Z \cdot V_{eff}$; (13)
According to normalization conditions, the density loss for ions with charge Z that are able to escape from the trap can be written as:

$$\Delta N_i = N_i \int_{E=E_b}^{\infty} f(E) dE \ , \qquad (14)$$

The energy loss due to escaping ions:

$$\Delta(N_i kT_i) = N_i \int_{E_i=E_b}^{\infty} (f_i(E_i) dE_i \, , \qquad (15)$$

The rate of diffusion escape from the trap for ions with charge Z is expressed as:

$$\frac{dN_i}{dt} = \nu_d \cdot \Delta N_i, \qquad (16)$$

and the rate of energy loss:

$$\frac{d(N_i kT_i)}{dt} = \nu_d \cdot \Delta(N_i kT_i) \ , \qquad (17)$$

where ν_d is the rate of diffusion escape perpendicular to the H direction and H the magnetic field strenghth.

The diffusion flux through the trap border /17/:

$$\Gamma = D_\perp \frac{\partial N_i}{\partial r} \ , \qquad (18)$$

where $D_\perp$ is the coefficient of perpendicular diffusion: $D_\perp = \frac{D}{1 + w_c^2 / \nu_i^2}$, D is the diffusion coefficient: $D = \frac{kT_i}{M_i \cdot \nu_i}$, ν_i is the total Coulomb collision rate for ith ionic species: $\nu_i = \sum_i \nu_{i,j}$, w_c is the ion cyclotron frequency for magnetic field induction B: $w_c = \frac{Z_i \cdot B}{M_i}$.

The ion escape speed can be written as:

$$\frac{dn_i}{dt} = 2\pi \cdot r_b \cdot L_{tr} \cdot \Gamma \ , \qquad (19)$$

where r_b is the electron beam radius and L_{tr} the effective trap length.

For uniform distribution of ions with charge Z in the trap, the rate of diffusion escape from the trap for ion densities reads as:

$$\frac{dN_i}{dt} = \frac{dn_i}{dt} / (\pi \cdot r_b^2 \cdot L_{tr}) = \frac{2}{r_b} \cdot \Gamma \ , \qquad (20)$$

If we suppose that ΔN_i=const at $0<r<r_b$ and it decreases linear to zero at $r_b<r<r_{td}$, where r_{td} is the drift tube radii, then:

$$\Gamma \sim D_\perp \cdot \frac{\Delta N_i}{(r_{td} - r_b)}, \qquad (21)$$

and the rate of diffusion escape:

$$v_d \sim \frac{2}{r_b \cdot (r_{td} - r_b)} \cdot D_\perp . \qquad (22)$$

Numerical model

Let the ionization proceed by single steps, then:

$$\begin{cases} \dfrac{dN_0}{dt} = -N_0\lambda_{0,1} + N_1\lambda_{1,0}, \\ \dfrac{dN_1}{dt} = N_0\lambda_{0,1} - N_1(\lambda_{1,2} + \lambda_{1,0}) + N_2\lambda_{2,1} - \left(\dfrac{dN_1}{dt}\right)^{radesc}, \\ \cdots\cdots\cdots\cdots\cdots\cdots\cdots\cdots \\ \dfrac{dN_i}{dt} = N_{i-1}\lambda_{i-1,i} - N_i(\lambda_{i,i+1} + \lambda_{i,i-1}) + N_{i+1}\lambda_{i+1,i} - \left(\dfrac{dN_i}{dt}\right)^{radesc}, \\ \dfrac{dN_Z}{dt} = N_{Z-1}\lambda_{Z-1,Z} - N_Z\lambda_{Z,Z-1} - \left(\dfrac{dN_Z}{dt}\right)^{radesc}, \end{cases} \qquad (23)$$

where N_0 .. N_Z are the ion and atom densities,
$\lambda_{0,1}$, $\lambda_{1,2}$, $\lambda_{i-1,i}$, $\lambda_{i,i+1}$, $\lambda_{Z-1,Z}$ are the ionization coefficients: $\lambda_{i,i+1} = \sigma_{i,i+1} j_e$,
$\lambda_{1,0}$, $\lambda_{2,1}$, $\lambda_{i+1,i}$, $\lambda_{i,i-1}$, $\lambda_{Z,Z-1}$ are the recombination and charge exchange coefficients:
$\lambda_{i,i-1}=\lambda_r+\lambda_p$,where $\lambda_r = \sigma_r \cdot j_e$, σ_r is the recombination cross-section,
$\lambda_p = \sigma_p \cdot N_0 \cdot \langle V_i \rangle$, σ_p is the charge exchange cross-section, N_0 is the density of neutral atoms, $\langle V_i \rangle$ is the mean ion speed.

The evolution of $N_i kT_i$ is described by:

$$\frac{d(N_i kT_i)}{dt} = N_{i-1}kT_{i-1}\lambda_{i-1,i} - N_i kT_i(\lambda_{i,i+1} + \lambda_{i,i-1}) + N_{i+1}kT_{i+1}\lambda_{i+1,i}$$

$$+\left[\frac{d(N_i kT_i)}{dt}\right]^{heating} + \sum_j \left[\frac{d(N_i kT_i)}{dt}\right]_j^{exchnge} - \left[\frac{d(N_i kT_i)}{dt}\right]^{radesc} . \qquad (24)$$

Calculations

At first, charge evolutions for the ionization of Kr atoms were calculated. Recombination, charge exchange, ion heating, energy exchange and ion escape processes were not taken into account. Relative Kr ion densities

calculated at j_e=1.2·10^{21} 1/(cm^2 ·s) , U_e=2·10^4 eV are shown in Fig. 1. We suppose that this consideration is true because our previous electron-impact cross-section measurements at big ion losses from the trap are in good agreement with theory. In these calculations the amount of ions was normalized to a unit magnitude for each time moment. This is the reason for us to calculate the charge-state evolution normalized to a unit magnitude for each time point.

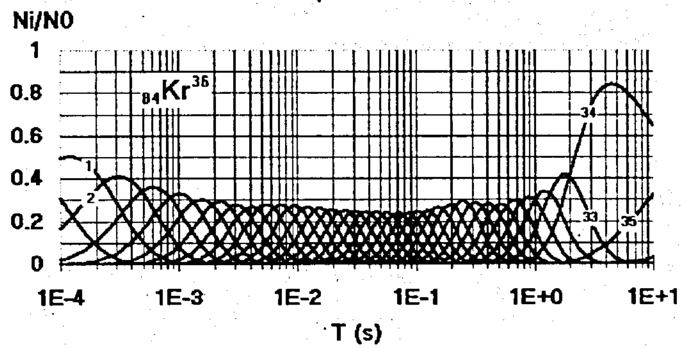

Fig. 1

The results were compared with those of analytical calculations carried out according to the analytical model of single step ionization /6/. It was noted that at a starting calculation step value of less than 4·10^{-5} s, the numerical data agree with the analytical ones.

Then the charge exchange processes were taken into account, and the calculations of charge exchange between Kr ions and Ne atoms were carried out for EBIS Krion-S electron beam parameters (the electron beam radius is 0.015 cm, j_e=1.2·10^{21} 1/(cm^2 ·s), U_e=7·10^3 eV). We suppose that the concentration of Ne atoms (N^0) in the electron beam is a constant because the average time of Ne atom pass through the electron beam diameter is about 5·10^{-6} s at an inside temperature of 4 K despite the average single-step ionization time of Ne atoms equal to 10^{-4} s. The time evolution of relative Kr ion densities at different Ne^0 concentrations is shown in Figs.2,3,4.

For Ne^0 concentration exceeding 10^7 cm^{-3}, the calculated results demonstrate a sufficient influence of charge exchange processes on relative concentrations of $Kr^{30+..34+}$ ions.

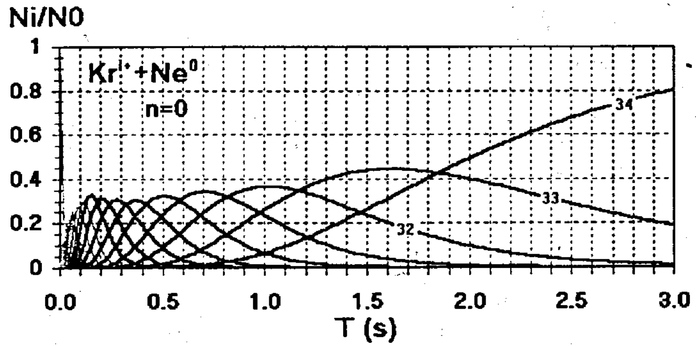

Fig. 2

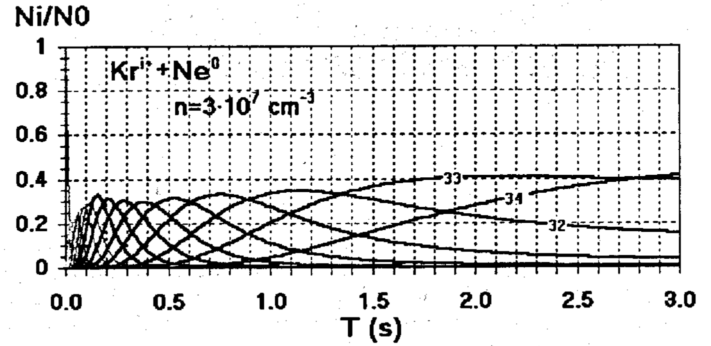

Fig. 3

The calculations of ion heating by the electron beam were performed at absolute density values with and without taking into account energy exchange and ion escape processes at j_e=1.2·10^{21} 1/(cm^2·s), U_e=7·10^3 eV, $N_{Kr}(0)$=10^9 cm^{-3}, r_p=0.015 cm, B=1.2 Tl. The average energy per Kr ion charge (kTi/Z) and the trap potential (V_{eff}) are the results of the calculation shown in Fig.5, where (kTi/Z) 1 and V_{eff} 1 correspond to the calculations without taking into account the ion escape process, (kTi/Z) 2, V_{eff} 2- with taking into account the one. In this case we assume that V_{eff}=$2V_b$.

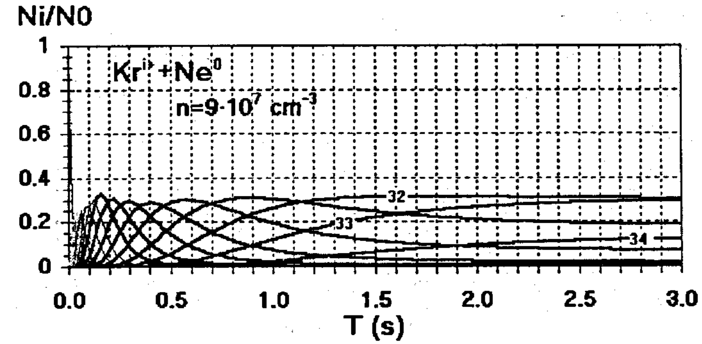

Fig. 4

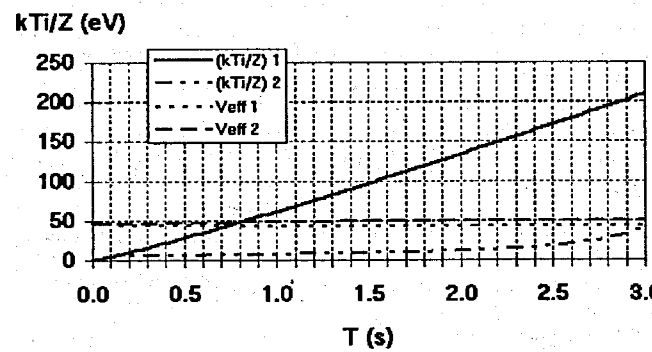

Fig. 5

Taking into account the ion escape process, the total Kr ion concentration decreased 3 orders in 3 s (see Fig. 7, dotted line 1).

The calculations without taking into account the ion escape process were carried out for Kr at j_e=1.2·10^{21} 1/(cm^2 ·s), U_e=7·10^3 eV, $N_{Kr}(0)$=10^9 cm^{-3}. The results presented as a function of j_e·t are shown in Fig.6.

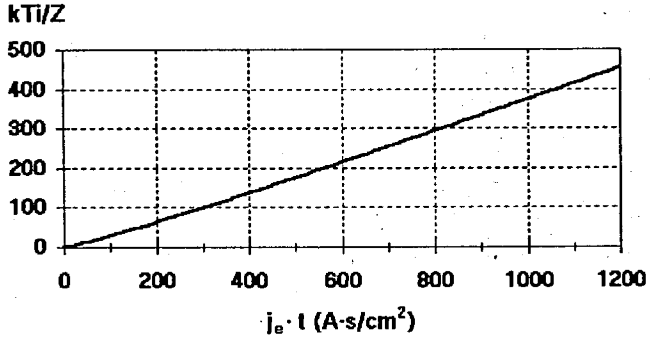

Fig. 6

The (kTi/Z) 1 results (Fig. 5) are applied to the results in Fig. 6.

The next step was to consider ion cooling processes. The method of ion cooling in EBIS was suggested by E.D. Donets and G.D. Shirkov/18/. Equation systems (23,24) created for Kr and Ne are solved simultaneously. The results for Kr at $j_e=1.2\cdot10^{21}$ 1/(cm^2·s), $U_e=7\cdot10^3$ eV, $N_{Kr}(0)=1.2\cdot10^{10}$ cm^{-3} and $N_{Kr}(0)=10^9$ cm^{-3} by cooling with Ne ions (the Ne atom concentration in the electron beam (N_{Ne}) is a constant and equal to $2.4\cdot10^6$ cm^{-3}) and without cooling are presented in Fig.7.

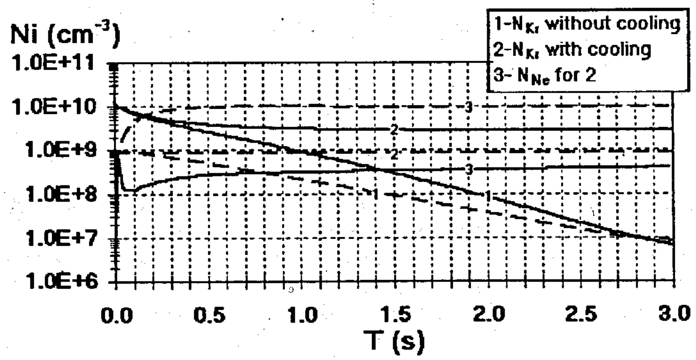

Fig. 7

The corresponding time dependences of beam compensation values are shown in Fig. 8, where the solid lines correspond to $N_{Kr}=1.2\cdot10^{10}$ cm^{-3} and the dotted ones to $N_{Kr}=10^9$ cm^{-3}.

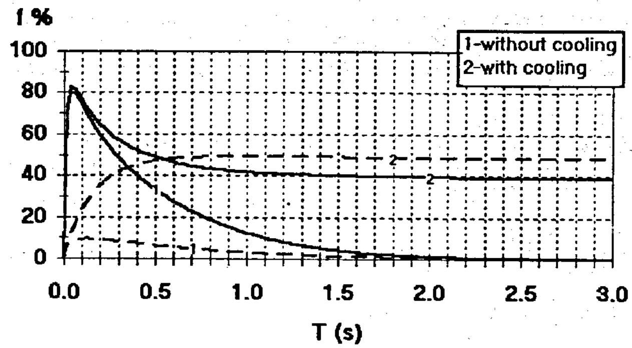

Fig. 8

Comparison with experimental results

The calculated results were compared with the experimental data of Kr current measurements at the EBIS Krion-S exit. The experimental current dependence on time was measured over an ion extraction time of 100 μs. The best numerical approximation was obtained at $V_{eff}=V_b$ for $j_e=1.77\cdot10^{21}$ 1/(cm^2·s), $U_e=7\cdot10^3$ eV, $N_{Kr}(0)=6\cdot10^9$ cm^{-3}, $r_p=0.015$ cm, B=1.2 Tl, by cooling with Ne ions. The results for output current are shown in Fig. 9.

The total numbers of ions, the values of beam compensation and the average ion temperatures corresponding to Fig. 9 are shown in Figs. 10,11,12.

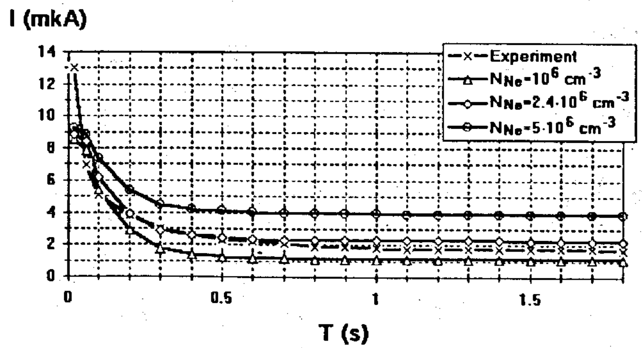

Fig. 9

The time evolution of Kr ion densities at $N_{Ne}=2.4\cdot10^6$ cm^{-3} corresponding to Fig. 9 is shown in Fig. 13. The results were confirmed by an experimental observation of Kr higher charge state evolution at the LU-20 output when the EBIS Krion-S was installed on the linac pre-injector /19/.

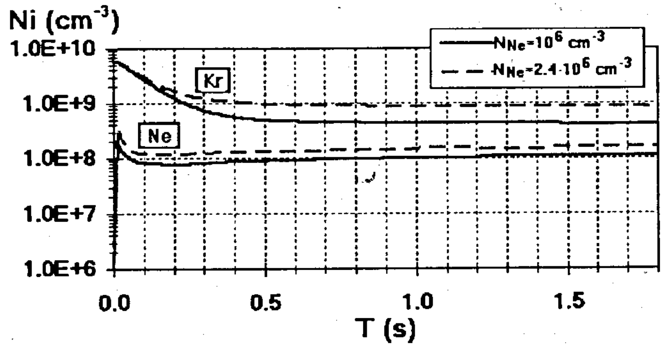

Fig. 10

Conclusion

The workable numerical model of EBIS has been created. The calculated results are close to the experimental ones. The model made more understandable the influence of different processes in the trap on the EBIS output parameters.

The authors are very grateful to Dr. E.D. Donets and Dr. G.D. Shirkov for their interest in the model and useful discussions.

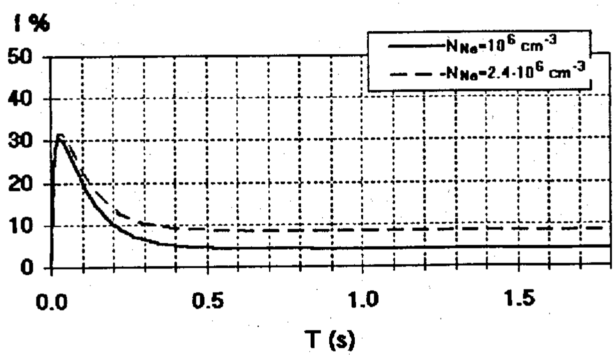

Fig. 11

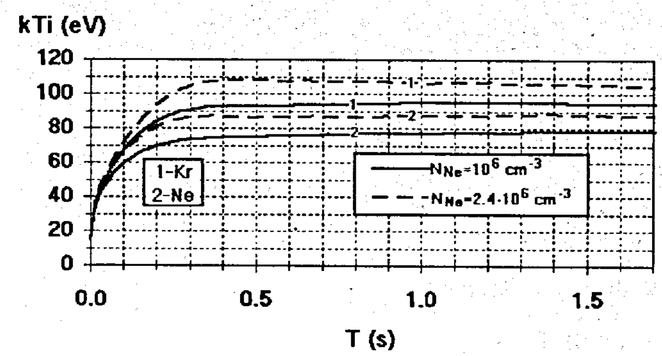

Fig. 12

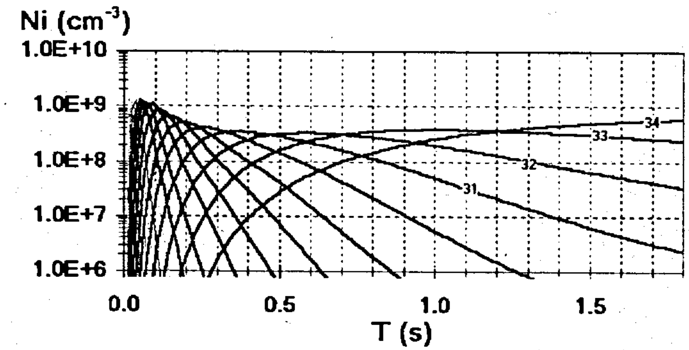

Fig. 13

References

1. E.D. Donets, Soviet Invention #248860 of 16.03.67, Bull. OIPOTZ, #24, p. 65, 1969
2. R. Becker in Proc. of the 2-nd EBIS Workshop, Saclay-Orsay, 185, 1981
3. M.C. Vella, Nucl. Instr. Meth. , 187, 313, 1981
4. M.A.Levine et al. Phys. Scripta, V T22, p. 157 , 1988
5. B.M.Penetrante et al. Phys. Rev., **A 43**, 4861 , 1991
6. B. Sh. Bochev et al. JINR Preprint P5-11566, 1978
7. B. Sh. Bochev et al. JINR Preprint P7-11567, 1978
8. W.Lotz, Z.Phys. **206**, p.205, 1967
9. W.Lotz, Z.Phys. **216**, p.241, 1968

10.E.D. Donets, A.I. Pikin, GTF, **70**, 6, 2025, 1976
11.Y.S.Kim and R.H. Pratt, Phys. Rev. **A 27**, 2913, 1983
12.A.Muller and E.Salzborn, Phys. Lett. **62A**, p.l391, 1977
13.Muller A. and Frodl R., Phys. Rev. **44** p.29 , 1980
14.Y.P.Raizer, Fizika gazovogo razriada, Moscow, "Nauka" , 1987
15.L.Spitzer, Physics of Fully Ionized Gases, Interscience, New York, 1956
16.J. Rose, M. Clark, Plasmas and Controlled Fusion, M.I.T. Press Massachusetts Institute of Technology and John Wiley & Sons, Inc., New York-London, 1961
17.Chen, Introduction to Plasma Physics and Controlled Fusion, Plenum Press New York and London, 1983
18.E.D. Donets, G.D. Shirkov, Soviet Invention #1225420 of 02.07.1984 Bul. #44, p. 69, 1989
19.I.V. Kalagin, V.P. Ovsyannikov, Book of Abstracts, ICIS'95, Wistler, BC, Canada, 1995